Analytical theory of effective interactions in binary colloidal systems of soft particles

M. Majka* and P. F. Góra

Marian Smoluchowski Institute of Physics, Jagiellonian University, Reymonta 4, 30-059 Kraków, Poland

(Received 24 July 2013; revised manuscript received 19 May 2014; published 16 September 2014)

While density functional theory with integral equations techniques are very efficient tools in the numerical analysis of complex fluids, analytical insight into the phenomenon of effective interactions is still limited. In this paper, we propose a theory of binary systems that results in a relatively simple analytical expression combining arbitrary microscopic potentials into effective interaction. The derivation is based on translating a many-particle Hamiltonian including particle-depletant and depletant-depletant interactions into the occupation field language, which turns the partition function into multiple Gaussian integrals, regardless of what microscopic potentials are chosen. As a result, we calculate the effective Hamiltonian and discuss when our formula is a dominant contribution to the effective interactions. Our theory allows us to analytically reproduce several important characteristics of systems under scrutiny. In particular, we analyze the following: the effective attraction as a demixing factor in the binary systems of Gaussian particles, the screening of charged spheres by ions, which proves equivalent to Derjaguin-Landau-Verwey-Overbeek (DLVO) theory, effective interactions in the binary mixtures of Yukawa particles, and the system of particles consisting of both a repulsive core and an attractive/repulsive Yukawa interaction tail. For this last case, we reproduce the "attraction-through-repulsion" and "repulsion-through-attraction" effects previously observed in simulations.

DOI: 10.1103/PhysRevE.90.032303 PACS number(s): 82.70.Dd, 89.75.Fb, 61.20.−p

I. INTRODUCTION

Effective interactions are of fundamental interest in the field of soft matter physics [1], especially in colloid studies. Their significance is enormous because they are essential for spontaneous self-organization, and they play a key role in polymer studies [1] as well as gel- and glass-forming research [2,3]. They are also important for molecular biophysics [4] and find multiple applications in nanotechnology [5]. Qualitatively similar phenomena of size separation are also encountered in vibrated granular matter research [6,7].

A comprehensive introduction to the contemporary theories of effective interactions can be found in [1,8,9]. The first successful description of effective interactions dates back to the research of Asakura and Oosawa [10,11], and later on to the work of Vrij [12]. Their approach, which was based on the consideration of excluded volume, is still used today, especially for nonspherical particles (e.g., [13,14]). At the advent of optical tweezers technology [15], effective interactions became accessible for direct measurements [16], which sparked a new interest in the systems for which the Asakura-Oosawa model proved insufficient.

One reason for violating the predictions of the Asakura-Oosawa model is that at high volume fraction packing, the system approaches a glassy transition, experiencing jammed dynamics. This is observed both experimentally [3,17,18] and via simulations [19–21]. On the other hand, systems with nontrivial or long-range interactions can be constructed. This includes charged particles [22], polymer-coated particles interacting via mushroom-like potentials [23], or polymer coils, which behave like soft, Gaussian-profiled particles [24]. The molecular-dynamics simulations for various combinations of repulsions and attractions have also shown that unexpected effects can be encountered, e.g., effective repulsion arising from attractive microscopic potentials or effective attraction induced by repulsive microscopic potentials [25].

A general theory capable of handling these phenomena has been proposed by Dijkstra *et al.* [26]. In their approach, a partition function for the system with arbitrarily chosen particle-depletant and depletant-depletant interaction is systematically expanded in terms of Mayer bond functions [1,8]. While this expansion is exact in principle, it is usually challenging to include high-order terms due to their mathematical form and nonperturbative character. Approximated techniques also exist based on integral equations, closure relations, and utilizing various density correlation functions [1,8]. Both tools have become a standard in the field, allowing the efficient numerical analysis of various systems, e.g., [24,27,28]. However, the analytical form of effective interactions is known only for several model systems (see [9] for review), and similar results for complex fluids are rather scarce (e.g., [29,30]).

While it is notoriously challenging to predict the effective interactions from arbitrary microscopic potentials, a simplified, tough analytical theory could find multiple applications in colloid research, e.g., in high-level solution design or in the context of Langevin dynamics simulation (e.g., [31–34]). In this paper, we propose such a theory, which offers both generality and comprehensible analytical form.

We consider a binary system of spherically symmetric particles with arbitrarily chosen microscopic potentials. In our approach, we introduce the so-called occupation functional (representing a number of particles at every position) and translate the semi-grand-canonical ensemble into the path-integral problem related to this functional. Regardless of microscopic potentials, this method turns the partition function into multiple Gaussian integrals. There are two major advantages of this transformation. On the one hand, we are able to identify and factorize a closed-form formula contributing to

*maciej.majka@uj.edu.pl

effective interactions, which is exact. On the other hand, we can approximate the effective Hamiltonian in order to identify further contributions and propose the criteria under which the exact part is dominant.

In our model, similar to [1] and [26], we consider two distinct species of particles in the D-dimensional volume $\Omega = L^D$. The system has temperature T, and we will denote $\beta = (k_B T)^{-1}$, where k_B is the Boltzmann constant. We will also use h to denote the Planck constant. In the system, there are N_1 particles of the first kind, and we denote the position and momentum of the ith particle with $\mathbf{R}_i$ and $\mathbf{P}_i$, respectively. The microscopic potential between these particles reads $U_{RR}(|\mathbf{R}_i - \mathbf{R}_j|)$, and effective interaction will be derived for this species. The second species, identified as depletant, consists of N_2 particles, which interact via potential $V(|\mathbf{r}_i - \mathbf{r}_j|)$, and their positions and momenta are denoted by $\mathbf{r}_i$ and $\mathbf{p}_i$. We will use the grand-canonical ensemble for depletant particles, so we associate a chemical potential μ with this species. Both types of particles cross-interact via the potential $U(|\mathbf{R}_i - \mathbf{r}_j|)$. The masses of colloid and depletant particles are m_1 and m_2, respectively. The total Hamiltonian of the system in its initial form has three contributions:

$$H_{\text{tot}} = H_{RR} + H_{rR} + H_{rr}, \tag{1}$$

where

$$H_{RR} = \sum_{i}^{N_1} \frac{\mathbf{P}_i^2}{2m_1} + \frac{1}{2} \sum_{\substack{i,j \\ i \neq j}}^{N_1} U_{RR}(|\mathbf{R}_i - \mathbf{R}_j|), \tag{2}$$

$$H_{rR} = \sum_{i}^{N_1} \sum_{j}^{N_2} U(|\mathbf{R}_i - \mathbf{r}_j|), \tag{3}$$

$$H_{rr} = \sum_{i}^{N_2} \frac{\mathbf{p}_i^2}{2m_2} + \frac{1}{2} \sum_{\substack{i,j \\ i \neq j}}^{N_2} V(|\mathbf{r}_i - \mathbf{r}_j|). \tag{4}$$

Let us introduce a pair of Fourier transforms:

$$\mathcal{U}(k) = \int_{\Omega} d\mathbf{r}\, e^{i\mathbf{k}\cdot\mathbf{r}} U(r),$$

$$\mathcal{V}(k) = \int_{\Omega} d\mathbf{r}\, e^{i\mathbf{k}\cdot\mathbf{r}} V(r).$$

We will show that effective interaction between a pair of colloid particles positioned at $\mathbf{R}_i$ and $\mathbf{R}_j$ has the following contribution:

$$U_{\text{eff}}(\mathbf{R}_i - \mathbf{R}_j) = -\frac{1}{(2\pi)^D} \int_{\tilde{\Omega}} d\mathbf{k}\, e^{i\mathbf{k}\cdot(\mathbf{R}_i - \mathbf{R}_j)} \frac{|\mathcal{U}(k)|^2}{\mathcal{V}(k)}. \tag{5}$$

This result is exact and sufficient to analytically reproduce many important characteristics of binary mixtures. This includes demixing of Gaussian particles, screening of charge in the system of charged spheres and ions, and "attraction-through-repulsion"/"repulsion-through-attraction" effects for particles characterized by a Yukawa interaction tail and a repulsive core. All of these effects were observed previously in simulations or described with various theories, but our approach provides a common framework for all of them, and our predictions are at least in qualitative agreement with existing results. By calculating the approximated form of the effective Hamiltonian, we will also show that there are other sources of effective interactions, and we will propose a criterion under which $U_{\text{eff}}(\mathbf{R}_i - \mathbf{R}_j)$ is dominant.

The paper is organized as follows: In Secs. II A–II C, we introduce our framework of occupation functional, in Sec. II D the formula for $U_{\text{eff}}(\mathbf{R}_i - \mathbf{R}_j)$ is derived, in Sec. II E the approximated partition functions is calculated, and Sec. II F concludes with the effective Hamiltonian and the accuracy of our model. The assumptions and caveats regarding the derivation are summarized in Sec. II G. Section III contains examples of applications for our theory. These includes the binary mixtures of Gaussian particles (Sec. III B), charged spheres in the presence of ions (Sec. III C), mixtures of Yukawa particles (Sec. III D), and mixtures of Yukawa particles with impenetrable cores (Sec. III E).

II. MODEL DERIVATION

A. System partition function

To begin the derivation of our model, we have to specify the partition function of the system. Our aim is to apply a new way to integrate out the depletant degrees of freedom. As a result, the effective Hamiltonian will be derived from the remaining expression. The initial Hamiltonian H_{tot} is defined by Eqs. (1)–(4). For this Hamiltonian, we introduce the mixed ensemble Ξ_{tot}, which is the grand-canonical ensemble for the depletant and the canonical ensemble for colloid particles. Written in standard space-momentum coordinates $\{\mathbf{P}_i, \mathbf{R}_i\}_{N_1}$ and $\{\mathbf{p}_i, \mathbf{r}_i\}_{N_2}$, the mixed ensemble can be regrouped in the following manner:

$$\Xi_{\text{tot}} = \prod_{i}^{N_1} \int d\mathbf{P}_i d\mathbf{R}_i \frac{\exp\left(-\beta(H_{RR} - \frac{1}{\beta}\ln \Xi)\right)}{N_1! h^{DN_1}}, \tag{6}$$

where

$$H_{\text{eff}} = H_{RR} - \frac{1}{\beta} \ln \Xi \tag{7}$$

is the effective Hamiltonian for the first species of particles, and

$$\Xi = \sum_{N_2=0}^{+\infty} \int d\mathbf{p}_i d\mathbf{r}_i \frac{\exp[-\beta(H_{rR} + H_{rr} - \mu N_2)]}{N_2! h^{DN_2}}. \tag{8}$$

According to [1], the term

$$U_{\text{eff}}^{\text{tot}} = -\frac{1}{\beta} \ln \Xi \tag{9}$$

acts as an additional potential, and this is the source of effective interactions. Therefore, calculating Ξ is of central interest for us.

First, it is feasible to rewrite H_{rr} in the following manner:

$$H_{rr} = \sum_{i}^{N_2} \frac{\mathbf{p}_i^2}{2m_2} + \frac{1}{2} \sum_{i,j}^{N_2} V(|\mathbf{r}_i - \mathbf{r}_j|) - \frac{N_2}{2} V(0), \tag{10}$$

which explicitly introduces $V(0)$. Another step is to integrate out depletant momenta $\mathbf{p}_j$, which allows us to rearrange Ξ into

the form

$$\Xi = \sum_{N_2} \frac{1}{L^{DN_2}} \prod_j^{N_2} \int d\mathbf{r}_j \frac{\exp[-\beta(\mathcal{H} - \tilde{\mu} N_2)]}{\Gamma(N_2 + 1)}, \quad (11)$$

where $\Gamma(\cdots)$ is the Euler Gamma function replacing the factorial, and

$$\mathcal{H} = \frac{1}{2} \sum_{i,j}^{N_2} V(|\mathbf{r}_i - \mathbf{r}_j|) + \sum_i^{N_1} \sum_j^{N_2} U(|\mathbf{R}_i - \mathbf{r}_j|), \quad (12)$$

$$\tilde{\mu} = \mu + \frac{1}{2} V(0) + \frac{D}{2\beta} \ln \frac{2\pi L^2 m_2}{\beta h^2}. \quad (13)$$

The partition function Ξ given in the form (11) is ready to be translated into the occupation field representation.

B. Occupation field representation

Let us consider a scalar field that assigns the number of depletant particles $\alpha(\mathbf{r})$ at certain position $\mathbf{r}$ to this position. The total number of depletant particles in the system reads

$$N_2 = \int_\Omega d\mathbf{r} \alpha(\mathbf{r}). \quad (14)$$

If $\alpha(\mathbf{r})$ particles occupy a position $\mathbf{r}$ and $\alpha(\mathbf{r}')$ particles occupy position $\mathbf{r}'$, then the energy of interaction between the sites $\mathbf{r}$ and $\mathbf{r}'$ is equal to $\alpha(\mathbf{r})\alpha(\mathbf{r}')V(|\mathbf{r} - \mathbf{r}'|)$. Therefore, we can use $\alpha(\mathbf{r})$ to translate interaction terms in the following manner:

$$\sum_{i,j}^{N_2} V(|\mathbf{r}_i - \mathbf{r}_j|) = \iint_\Omega d\mathbf{r}\, d\mathbf{r}' \alpha(\mathbf{r})\alpha(\mathbf{r}')V(|\mathbf{r} - \mathbf{r}'|), \quad (15)$$

$$\sum_i^{N_1} \sum_j^{N_2} U(|\mathbf{R}_i - \mathbf{r}_j|) = \sum_i^{N_1} \int_\Omega d\mathbf{r}\, \alpha(\mathbf{r}) U(|\mathbf{R}_i - \mathbf{r}|). \quad (16)$$

In principle, $\alpha(\mathbf{r})$ takes only discrete values $0, 1, 2, \ldots$, but we will allow it to vary continuously.

The formulas (14)–(16) suggest that we can understand $\mathcal{H}$ and N_2 as the functionals of $\alpha(\mathbf{r})$. In turn, we could replace the multiple integrations in (11) with a functional integral with respect to $\alpha(\mathbf{r})$, namely

$$\Xi \to \int \mathcal{D}[\alpha] \frac{\exp[-\beta(\mathcal{H} - \tilde{\mu} N_2)]}{\Gamma(N_2 + 1)}. \quad (17)$$

The path integral can be specified as the integral with respect to the Fourier series coefficients of $\alpha(\mathbf{r})$ [35]:

$$\alpha(\mathbf{r}) = \frac{1}{\Omega} \sum_{\mathbf{n} \in Z^D} a_n e^{i \frac{2\pi}{L} \mathbf{n} \cdot \mathbf{r}}. \quad (18)$$

Here $\mathbf{n}$ is a D-dimensional vector, whose components vary discretely from $-\infty$ to $+\infty$. Therefore, we shall denote the set of index vectors $\mathbf{n}$ with Z^D. The Fourier series expansion of $\alpha(\mathbf{r})$ requires us to assume periodic boundary conditions. Since the field $\alpha(\mathbf{r})$ is real, the symmetry $a_{-\mathbf{n}} = a_{\mathbf{n}}^*$ is also required. The a_0 coefficient has a special interpretation:

$$a_0 = \int_\Omega d\mathbf{r}\, \alpha(\mathbf{r}) = N_2. \quad (19)$$

Additionally, we have to assume that potentials $U(\mathbf{r})$ and $V(\mathbf{r})$ are also periodic over length L, which should be of little influence if the range of those potentials is much shorter than L. If so, then the Fourier series expansion (18) simplifies the interaction terms:

$$\iint_\Omega d\mathbf{r}\, d\mathbf{r}' \alpha(\mathbf{r})\alpha(\mathbf{r}')V(|\mathbf{r} - \mathbf{r}'|) = \frac{1}{\Omega} \sum_{\mathbf{n} \in Z^D} |a_\mathbf{n}|^2 \mathcal{V}_\mathbf{n}, \quad (20)$$

$$\sum_i^{N_1} \int_\Omega d\mathbf{r}\, \alpha(\mathbf{r}) U(|\mathbf{R}_i - \mathbf{r}|) = \frac{1}{\Omega} \sum_{\mathbf{n} \in Z^D} a_\mathbf{n} \sum_i \mathcal{U}_\mathbf{n}^{(i)}, \quad (21)$$

where

$$\mathcal{V}_\mathbf{n} = \int_\Omega d\mathbf{r}\, e^{i \frac{2\pi}{L} \mathbf{n} \cdot \mathbf{r}} V(r), \quad (22)$$

$$\mathcal{U}_\mathbf{n}^{(i)} = \int_\Omega d\mathbf{r}\, e^{i \frac{2\pi}{L} \mathbf{n} \cdot \mathbf{r}} U(|\mathbf{R}_i - \mathbf{r}|). \quad (23)$$

From these formulas, it follows that

$$\mathcal{H} - \tilde{\mu} N_2 = \frac{1}{2\Omega} \sum_{\mathbf{n} \in Z^D} |a_\mathbf{n}|^2 \mathcal{V}_\mathbf{n} + \frac{1}{\Omega} \sum_{\mathbf{n} \in Z^D} a_\mathbf{n} \left(\sum_i \mathcal{U}_\mathbf{n}^{(i)} - \tilde{\mu} \Omega \delta_{\mathbf{n},0} \right), \quad (24)$$

which can be further rearranged into

$$\mathcal{H} - \tilde{\mu} N_2 = \sum_{\mathbf{n} \in Z^D} \frac{\mathcal{V}_\mathbf{n}}{2\Omega} \left| a_\mathbf{n} + \frac{\sum_i \mathcal{U}_{-\mathbf{n}}^{(i)} - \tilde{\mu} \Omega \delta_{\mathbf{n},0}}{\mathcal{V}_\mathbf{n}} \right|^2 - \sum_{\mathbf{n} \in Z^D} \frac{\left| \sum_i \mathcal{U}_\mathbf{n}^{(i)} - \tilde{\mu} \Omega \delta_{\mathbf{n},0} \right|^2}{2\Omega \mathcal{V}_\mathbf{n}}, \quad (25)$$

and finally the path integral is specified as

$$\Xi = \prod_{\mathbf{n} \in Z^D} \int da_\mathbf{n} \frac{\exp[-\beta(\mathcal{H} - \tilde{\mu} N_2)]}{\Gamma(a_0 + 1)}. \quad (26)$$

In the above formula, we intentionally omit writing the limits of integration since they need to be discussed in greater detail in the following section.

C. Non-negative fields from Fourier modes

In principle, the occupation field $\alpha(\mathbf{r})$ should be non-negative. Unfortunately, a field constructed according to (18) from the arbitrarily chosen values of $a_\mathbf{n}$ does not necessarily meet this requirement. However, it is always true that $a_0 \geqslant 0$, since it is the number of depletant particles. Therefore, for any values of $a_{\mathbf{n} \neq 0}$ we can choose a_0 such that $\alpha(\mathbf{r})$ is non-negative. More precisely, we can write

$$\tilde{\alpha}(\mathbf{r}) = \sum_{\mathbf{n} \in Z^D \setminus 0} a_\mathbf{n} e^{i \frac{2\pi}{L} \mathbf{n} \cdot \mathbf{r}}, \quad (27)$$

where $\setminus 0$ indicates the exclusion of a_0. $\tilde{\alpha}(\mathbf{r})$ is a real function and, necessarily,

$$\int_\Omega d\mathbf{r}\, \tilde{\alpha}(\mathbf{r}) = 0. \quad (28)$$

This property means that $\tilde{\alpha}(\mathbf{r})$ has to take both negative and non-negative values for different $\mathbf{r}$, so integral (28) is 0. Therefore, there must exist a global minimum of $\tilde{\alpha}(\mathbf{r})$, and $\tilde{\alpha}(\mathbf{r})$ is negative in this minimum. Finally, for

$$a_0 \geqslant M = -\min_{\mathbf{r}}[\tilde{\alpha}(\mathbf{r})], \tag{29}$$

the occupation field $\alpha(\mathbf{r})$ is non-negative. Here, we denote the global minimum of $\tilde{\alpha}(\mathbf{r})$ with respect to $\mathbf{r}$ by $\min_{\mathbf{r}}[\tilde{\alpha}(\mathbf{r})]$. The limit M can be also rewritten in the following form:

$$M = -\sum_{\mathbf{n}\in Z^D\setminus 0} a_{\mathbf{n}} e^{i\frac{2\pi}{L}\mathbf{n}\cdot\mathbf{r}(a_{\mathbf{n}})}, \tag{30}$$

where $\mathbf{r}(a_{\mathbf{n}})$ is the position of the global minimum as a function of $a_{\mathbf{n}}$. Formally, $\mathbf{r}(a_{\mathbf{n}})$ can be determined from the equation

$$\nabla_{\mathbf{r}} \sum_{\mathbf{n}\in Z^D\setminus 0} a_{\mathbf{n}} e^{i\frac{2\pi}{L}\mathbf{n}\cdot\mathbf{r}} = 0. \tag{31}$$

Concluding this section, we can choose the limits of integration for $a_{\mathbf{n}\neq 0}$ as $\pm\infty$ and the limits for a_0 as $[M, +\infty)$. However, M is now a function of $a_{\mathbf{n}\neq 0}$, which fixes the order of integrals in (26). Let us combine (25) and (26) to write Ξ in the following form:

$$\Xi = e^{-\beta\Phi} \prod_{\mathbf{n}\in Z^D\setminus 0} I_{\mathbf{n}} I_0(M), \tag{32}$$

in which

$$\Phi = -\sum_{\mathbf{n}\in Z^D} \frac{\left|\sum_i \mathcal{U}_{\mathbf{n}}^{(i)} - \tilde{\mu}\Omega\delta_{\mathbf{n},0}\right|^2}{2\Omega\mathcal{V}_{\mathbf{n}}} \tag{33}$$

and

$$I_{\mathbf{n}\neq 0} = \int_{-\infty}^{+\infty} da_{\mathbf{n}} \exp\left(-\frac{\beta\mathcal{V}_{\mathbf{n}}}{2\Omega}\left|a_{\mathbf{n}} + \frac{\sum_i \mathcal{U}_{-\mathbf{n}}^{(i)}}{\mathcal{V}_{\mathbf{n}}}\right|^2\right), \tag{34}$$

$$I_0(M) = \int_M^{+\infty} da_0 \frac{\exp\left(-\frac{\beta\mathcal{V}_0}{2\Omega}\left|a_0 + \frac{\sum_i \mathcal{U}_0^{(i)} - \tilde{\mu}\Omega}{\mathcal{V}_0}\right|^2\right)}{\Gamma(a_0+1)}. \tag{35}$$

For the sake of more compact notation, we will denote

$$c_{\mathbf{n}} = \frac{\sum_i \mathcal{U}_{-\mathbf{n}}^{(i)} - \tilde{\mu}\Omega\delta_{0\mathbf{n}}}{\mathcal{V}_{\mathbf{n}}}, \quad \gamma_{\mathbf{n}} = \frac{\beta\mathcal{V}_{\mathbf{n}}}{2\Omega}. \tag{36}$$

D. The effective interaction

In this section, we will identify the exact part of effective interactions. We substitute now (32) into the formula for $U_{\text{eff}}^{\text{tot}}$, namely

$$U_{\text{eff}}^{\text{tot}} = -\frac{1}{\beta}\ln\Xi = \Phi - \frac{1}{\beta}\ln\left(\prod_{\mathbf{n}\in Z^D\setminus 0} I_{\mathbf{n}} I_0(M)\right). \tag{37}$$

We will show that Φ gives rise to the effective interaction $U_{\text{eff}}(|\mathbf{R}_i - \mathbf{R}_j|)$. Expanding (33) and taking advantage of the Kronecker δ, we arrive at

$$\Phi = -\sum_{i\neq j}\sum_{\mathbf{n}\in Z^D} \frac{\mathcal{U}_{\mathbf{n}}^{(i)}\mathcal{U}_{-\mathbf{n}}^{(j)}}{2\Omega\mathcal{V}_{\mathbf{n}}} - \sum_i \sum_{\mathbf{n}\in Z^D} \frac{\left|\mathcal{U}_{\mathbf{n}}^{(i)}\right|^2}{2\Omega\mathcal{V}_{\mathbf{n}}} + \frac{2\tilde{\mu}\sum_i \mathcal{U}_0^{(i)} - \tilde{\mu}^2\Omega}{2\mathcal{V}_0}. \tag{38}$$

To process the three terms in Φ, one can notice that

$$\begin{aligned}\mathcal{U}_{\mathbf{n}}^{(i)} &= \int_\Omega d\mathbf{r}\, e^{i\frac{2\pi}{L}\mathbf{n}\cdot\mathbf{r}} U(|\mathbf{R}_i - \mathbf{r}|) \\ &= e^{i\frac{2\pi}{L}\mathbf{n}\cdot\mathbf{R}_i} \int_{\Omega_i} d\mathbf{r}\, e^{i\frac{2\pi}{L}\mathbf{n}\cdot\mathbf{r}} U(r) \\ &= e^{i\frac{2\pi}{L}\mathbf{n}\cdot\mathbf{R}_i} \mathcal{U}\left(\frac{2\pi}{L}\mathbf{n}\right).\end{aligned} \tag{39}$$

Here Ω_i is a volume shifted by $\mathbf{R}_i$. In the continuous limit of huge volume $L \to +\infty$, we can substitute $\mathbf{k} = \frac{2\pi}{L}\mathbf{n}$, so

$$\mathcal{U}_{\mathbf{n}}^{(i)} \to e^{i\mathbf{k}\cdot\mathbf{R}_i}\mathcal{U}(\mathbf{k}). \tag{40}$$

Further, $\sum_{\mathbf{n}} \to \frac{\Omega}{(2\pi)^D}\int_{\tilde{\Omega}}$ and $\Omega_i \to \Omega$, so $\mathcal{U}(\mathbf{k})$ becomes a Fourier transform of $U(r)$. Similar considerations allow us to transform $\mathcal{V}_{\mathbf{n}}$ into $\mathcal{V}(\mathbf{k})$. Finally, in the continuous limit,

$$\begin{aligned}-\sum_{\mathbf{n}\in Z^D} \frac{\mathcal{U}_{\mathbf{n}}^{(i)}\mathcal{U}_{-\mathbf{n}}^{(j)}}{\Omega\mathcal{V}_{\mathbf{n}}} &\to -\frac{1}{(2\pi)^D}\int_{\tilde{\Omega}} d\mathbf{k}\, e^{i\mathbf{k}\cdot(\mathbf{R}_i - \mathbf{R}_j)} \frac{|\mathcal{U}(\mathbf{k})|^2}{\mathcal{V}(\mathbf{k})} \\ &= U_{\text{eff}}(\mathbf{R}_i - \mathbf{R}_i).\end{aligned} \tag{41}$$

Formula (41) constitutes the main result of this paper, which is the expression for the effective interaction between two particles. Having established this result, it follows that

$$-\sum_i \sum_{\mathbf{n}\in Z^D} \frac{\left|\mathcal{U}_{\mathbf{n}}^{(i)}\right|^2}{\Omega\mathcal{V}_{\mathbf{n}}} \to \sum_i U_{\text{eff}}(0) = N_1 U_{\text{eff}}(0) \tag{42}$$

and

$$\frac{2\tilde{\mu}\sum_i \mathcal{U}_0^{(i)} - \tilde{\mu}^2\Omega}{2\mathcal{V}_0} \to \frac{2\tilde{\mu}N_1\mathcal{U}(0) - \Omega\tilde{\mu}^2}{2\mathcal{V}(0)}. \tag{43}$$

In summary, we conclude that the general form of Φ reads

$$\Phi = \frac{1}{2}\sum_{i\neq j}^{N_1} U_{\text{eff}}(\mathbf{R}_i - \mathbf{R}_j) + \frac{N_1}{2}U_{\text{eff}}(0) + \frac{2\tilde{\mu}N_1\mathcal{U}(0) - \Omega\tilde{\mu}^2}{2\mathcal{V}(0)}. \tag{44}$$

Immediately one can recognize that we have obtained the effective interaction between every pair of particles, which is expected for the multiparticle system. This result is exact up to the approximations required to introduce the occupation number functional.

E. Approximated calculation of $\ln\prod I_{\mathbf{n}} I_0(M)$

Having found Φ, we would also like to calculate the $\prod I_{\mathbf{n}} I_0(M)$ to obtain the effective Hamiltonian. However, this can be completed only via certain approximations.

First of all, let us recall that, according to (35), $I_0(M)$ reads

$$I_0(M) = \int_M^{+\infty} da_0 \frac{e^{-\gamma_0(a_0+c_0)^2}}{\Gamma(a_0+1)}.$$

In principle M is non-negative, and for such an argument $I_0(M)$ is a decreasing function, reaching asymptotically 0 in the limit of $M \to +\infty$. $I_0(M)$ can have a well-defined kink at $M = -c_0$, provided that $c_0 < 0$ and $\gamma_0 \gg 1$. We will

approximate now $I_0(M)$ up to first order in the logarithmic derivative, namely

$$I_0(M) = \exp\left(\ln I_0(0) + \frac{I_0'(0)}{I_0(0)}M + \cdots\right) \simeq I_0(0)e^{\frac{I_0'(0)}{I_0(0)}M}. \tag{45}$$

This is accurate provided that there is no kink for $M \in [0, +\infty)$, which requires that $c_0 > 0$. For more compact notation, we denote

$$\mathcal{I}_0 = \frac{I_0'(0)}{I_0(0)}. \tag{46}$$

Under approximation (45) and using expansion (30) for M, we can write

$$\prod_{\mathbf{n}\in Z^D\setminus 0} I_{\mathbf{n}} I_0(M) \approx \prod_{\mathbf{n}\in Z^D\setminus 0} \int_{-\infty}^{+\infty} da_{\mathbf{n}} I_0(0) \times \exp\left(-\gamma_{\mathbf{n}}|a_{\mathbf{n}} + c_{\mathbf{n}}|^2 - \mathcal{I}_0 a_{\mathbf{n}} e^{i\frac{2\pi}{L}\mathbf{n}\cdot\mathbf{r}(a_{\mathbf{n}})}\right). \tag{47}$$

This expression is still dependent on $\mathbf{r}(a_{\mathbf{n}})$, which is an implicit function of $a_{\mathbf{n}}$. To proceed, we will approximate $\mathbf{r}(a_{\mathbf{n}})$ by a constant value. One can notice that the quadratic term in (47) has the extreme value for $a_{\mathbf{n}} = -c_{\mathbf{n}}$, and we expect that the integral (47) is dominated by the contribution from $a_{\mathbf{n}} \approx -c_{\mathbf{n}}$. Let us transform the integration variables,

$$\Delta a_{\mathbf{n}} = a_{\mathbf{n}} + c_{\mathbf{n}}, \tag{48}$$

and approximate M in the vicinity of $c_{\mathbf{n}}$ up to first order in $\Delta a_{\mathbf{n}}$:

$$-\sum_{\mathbf{n}\in Z^D\setminus 0} a_{\mathbf{n}} e^{i\frac{2\pi}{L}\mathbf{n}\cdot\mathbf{r}(a_{\mathbf{n}})} \simeq \sum_{\mathbf{n}\in Z^D\setminus 0} (c_{\mathbf{n}} - \Delta a_{\mathbf{n}}) e^{i\frac{2\pi}{L}\mathbf{n}\cdot\mathbf{r}(c_{\mathbf{n}})}. \tag{49}$$

Now, (47) turns into

$$\prod_{\mathbf{n}\in Z^D\setminus 0} I_{\mathbf{n}} I_0(M) \approx \prod_{\mathbf{n}\in Z^D\setminus 0} \exp\left(\mathcal{I}_0 c_{\mathbf{n}} e^{i\frac{2\pi}{L}\mathbf{n}\cdot\mathbf{r}(c_{\mathbf{n}})}\right) I_0(0) \times \int_{-\infty}^{+\infty} d\Delta a_{\mathbf{n}} \exp\left(-\gamma_{\mathbf{n}}|\Delta a_{\mathbf{n}}|^2 - \mathcal{I}_0 \Delta a_{\mathbf{n}} e^{i\frac{2\pi}{L}\mathbf{n}\cdot\mathbf{r}(c_{\mathbf{n}})}\right). \tag{50}$$

We can rearrange the quadratic expression in the exponent of (50),

$$\sum_{\mathbf{n}\in Z^D\setminus 0} \gamma_{\mathbf{n}}|\Delta a_{\mathbf{n}}|^2 + \mathcal{I}_0 \sum_{\mathbf{n}\in Z^D\setminus 0} \Delta a_{\mathbf{n}} e^{i\frac{2\pi}{L}\mathbf{n}\cdot\mathbf{r}(c_{\mathbf{n}})} = \sum_{\mathbf{n}\in Z^D\setminus 0} \gamma_{\mathbf{n}} \left|\Delta a_{\mathbf{n}} + \mathcal{I}_0 \frac{e^{-i\frac{2\pi}{L}\mathbf{n}\cdot\mathbf{r}(c_{\mathbf{n}})}}{2\gamma_{\mathbf{n}}}\right|^2 - \sum_{\mathbf{n}\in Z^D\setminus 0} \frac{\mathcal{I}_0^2}{4\gamma_{\mathbf{n}}}. \tag{51}$$

Finally, since the integration variable $\Delta a_{\mathbf{n}}$ is complex, we introduce its polar parametrization:

$$\rho_{\mathbf{n}} e^{\pm\imath\phi_{\mathbf{n}}} = \Delta a_{\pm\mathbf{n}} + \mathcal{I}_0 \frac{e^{\mp i\frac{2\pi}{L}\mathbf{n}\cdot\mathbf{r}(c_{\mathbf{n}})}}{2\gamma_{\pm\mathbf{n}}}. \tag{52}$$

Once (51) and (52) are applied to (50), the integrations can be performed, provided that all $\mathrm{Re}(\gamma_{\mathbf{n}}) > 0$. The result reads

$$\ln \prod_{\mathbf{n}\in Z^D\setminus 0} I_{\mathbf{n}} I_0(M) \approx \ln I_0(0) + \sum_{\mathbf{n}\in Z^D\setminus 0} \ln\frac{\pi}{\gamma_{\mathbf{n}}} + \mathcal{I}_0 \sum_{\mathbf{n}\in Z^D\setminus 0} c_{\mathbf{n}} e^{i\frac{2\pi}{L}\mathbf{n}\cdot\mathbf{r}(c_{\mathbf{n}})} + \sum_{\mathbf{n}\in Z^D\setminus 0} \frac{\mathcal{I}_0^2}{4\gamma_{\mathbf{n}}}. \tag{53}$$

F. Effective Hamiltonian and model accuracy

Let us summarize the two preceding sections. Getting back to the formula (7), the effective Hamiltonian of the entire system reads

$$H_{\mathrm{eff}} = H_{RR} + \Phi - \frac{1}{\beta}\ln \prod_{\mathbf{n}\in Z^D\setminus 0} I_{\mathbf{n}} I_0(M).$$

Turning (53) into its continuous form, we obtain the final expression for the effective Hamiltonian:

$$H_{\mathrm{eff}} \approx H_{RR} + \Phi - \frac{1}{\beta}\left(\frac{\Omega}{(2\pi)^D}\int_{\tilde{\Omega}} d\mathbf{k} \ln\frac{\pi}{\gamma(\mathbf{k})} + \frac{\mathcal{I}_0\Omega}{(2\pi)^D}\sum_i^{N_1}\int_{\tilde{\Omega}} d\mathbf{k}\, e^{i\mathbf{k}\cdot(\mathbf{r}_{\min}-\mathbf{R}_i)}\frac{\mathcal{U}(\mathbf{k})}{\mathcal{V}(\mathbf{k})} - \frac{N_1\mathcal{I}_0\mathcal{U}(0)}{\mathcal{V}(0)} + \frac{\mathcal{I}_0^2\Omega}{4(2\pi)^D}\int_{\tilde{\Omega}} d\mathbf{k}\frac{1}{\gamma(\mathbf{k})} - \frac{\mathcal{I}_0^2}{4\gamma(0)} + \ln\frac{\gamma(0)I_0(0)}{\pi}\right), \tag{54}$$

where $r_{\min}$ is the global minimum, found from the equation

$$\nabla_{\mathbf{r}} \sum_i^{N_1}\int_{\tilde{\Omega}} d\mathbf{k} e^{i\mathbf{k}\cdot(\mathbf{r}-\mathbf{R}_i)}\frac{\mathcal{U}(\mathbf{k})}{\mathcal{V}(\mathbf{k})} = 0. \tag{55}$$

Furthermore, according to (44), the exact part of H_{eff} reads

$$\Phi = \frac{1}{2}\sum_{i\neq j}^{N_1} U_{\mathrm{eff}}(\mathbf{R}_i - \mathbf{R}_j) + \frac{N_1}{2}U_{\mathrm{eff}}(0) + \frac{2\tilde{\mu}N_1\mathcal{U}(0) - \Omega\tilde{\mu}^2}{2\mathcal{V}(0)},$$

where the effective interaction $U_{\mathrm{eff}}(\mathbf{R}_i - \mathbf{R}_j)$ is defined by (41).

Let us scrutinize the following term from H_{eff}:

$$\Delta U_{\mathrm{eff}} = \frac{1}{\beta}\frac{\mathcal{I}_0\Omega}{(2\pi)^D}\sum_i^{N_1}\int_{\tilde{\Omega}} d\mathbf{k}\, e^{i\mathbf{k}\cdot(\mathbf{r}_{\min}-\mathbf{R}_i)}\frac{\mathcal{U}(\mathbf{k})}{\mathcal{V}(\mathbf{k})}. \tag{56}$$

First of all, this term is an explicit function of $\mathbf{R}_i$, which is in stark contrast to the Mayer bond expansion, in which such terms are excluded. This exclusion is motivated by the conservation of energy when the entire system is translated [1]. However, in our case, the global translation $\mathbf{R}_i \to \mathbf{R}_i + \delta$ yields $\mathbf{r}_{\min} \to \mathbf{r}_{\min} + \delta$, thus (56) is, in fact, translationally invariant.

Secondly, one can notice that since $\mathbf{r}_{\min}$ is a function of $\mathbf{R}_i$ itself, there is possibly an additional effective interaction embedded in ΔU_{eff}. Therefore, $U_{\mathrm{eff}}(\mathbf{R}_i - \mathbf{R}_j)$ is the dominant source of effective interactions provided that

$$U_{\mathrm{eff}}(\mathbf{R}_i - \mathbf{R}_j) \gg \Delta U_{\mathrm{eff}}. \tag{57}$$

Whether this relation is satisfied depends on both thermodynamic parameters and the choice of microscopic potentials, which makes it difficult to analyze in a general case. However,

if this relation is seriously violated, one might attempt to estimate the influence of $\Delta U_{\rm eff}$ on effective interactions from the following reasoning:

$$|\Delta U_{\rm eff}| < \frac{1}{\beta}\frac{\mathcal{I}_0\Omega}{(2\pi)^D}\int_{\tilde\Omega} d\mathbf{k}\sqrt{\left|\sum_i^{N_1} e^{i\mathbf{k}\cdot(\mathbf{r}_{\rm min}-\mathbf{R}_i)}\frac{\mathcal{U}(\mathbf{k})}{\mathcal{V}(\mathbf{k})}\right|^2}$$
$$= \frac{N_1^{1/2}}{\beta}\frac{\mathcal{I}_0\Omega}{(2\pi)^D}\int_{\tilde\Omega} d\mathbf{k}\left|\frac{\mathcal{U}(\mathbf{k})}{\mathcal{V}(\mathbf{k})}\right|\sqrt{1+\sum_{i\neq j}^{N_1}\frac{e^{i\mathbf{k}\cdot(\mathbf{R}_j-\mathbf{R}_i)}}{N_1}}$$
$$\simeq \frac{1}{\beta}\frac{\mathcal{I}_0\Omega}{(2\pi)^D}\left(N_1^{1/2}\int_{\tilde\Omega} d\mathbf{k}\left|\frac{\mathcal{U}(\mathbf{k})}{\mathcal{V}(\mathbf{k})}\right| + \frac{1}{2N_1^{1/2}}\sum_{i\neq j}^{N_1}\int_{\tilde\Omega} d\mathbf{k}\, e^{i\mathbf{k}\cdot(\mathbf{R}_j-\mathbf{R}_i)}\left|\frac{\mathcal{U}(\mathbf{k})}{\mathcal{V}(\mathbf{k})}\right|\right). \quad (58)$$

This formula also predicts the effective interactions, though we expect it to be overestimated in this case.

G. Caveats

Throughout the derivation section, we introduced numerous concepts, assumptions, and approximations. We would like to list these now and discuss their validity.

One general concern is related to path integrals. We allow $\alpha(\mathbf{r})$ to vary continuously, while the number of particles at every position should be integer. This means that the discretely varying trajectories, which are physically meaningful, are given infinitesimally small statistical weights. This might result in losing some important characteristics, similarly to the Bose-Einstein condensation, which is lost if the discrete partition function is replaced with the continuous one without proper care [40]. This problem has yet to be investigated.

Further, let us explicitly recall that the total effective potential has two parts, Φ and $-\frac{1}{\beta}\ln\prod_{\mathbf{n}\in Z^D\setminus 0} I_{\mathbf{n}} I_0(M)$. While we show in Sec. III that Φ is enough to reproduce many desired characteristics of effective interactions, there is no guarantee that the other part can be neglected in particular conditions. This is caused by the approximations applied in Sec. II E. The logarithmic expansion (45) in M is accurate provided that $c_0 > 0$, or, explicitly,

$$N_1\mathcal{U}(0) > \tilde\mu\Omega. \quad (59)$$

Satisfying this relation requires a high N_1 in a small volume Ω, but there is a risk of falling into the range of thermodynamic parameters relevant for a crystal or glassy state. Alternatively, the concentration of depletant might be low, which should entail low $\tilde\mu$, but the exact dependence of $\tilde\mu$ on average N_2 is as difficult to establish as $H_{\rm eff}$. If (59) is not satisfied (so $c_0 < 0$), then (45) works well for $M < -c_0$, but it loses accuracy for $M > -c_0$. Another issue is the expansion (49), linearizing M in the vicinity of $c_{\mathbf{n}}$. Since each $I_{\mathbf{n}\neq 0}$ is the integral of a Gaussian centered at $c_{\mathbf{n}}$, this expansion is justified, but the control over its accuracy is lost as the width of the Gaussian grows. Unfortunately, this is exactly the case for high-order $I_{\mathbf{n}}$, since we expect $\gamma_{\mathbf{n}} \to 0$ for large n.

Yet another concern is whether the depletant-depletant potential can have a negative or partially negative Fourier transform. Since each $I_{\mathbf{n}\neq 0}$ is the Gaussian integral, it would be divergent for $\mathcal{V}_{\mathbf{n}} < 0$, hence $\prod I_{\mathbf{n}} I_0(M) \to +\infty$. In this case, $H_{\rm eff}$ given by (54) is meaningless, but we will argue that Φ might still provide some useful information. In general, it is true that

$$\ln I_{\mathbf{n}} I_0(M) \leqslant \ln I_{\mathbf{n}} I_0(0) = \sum_{\mathbf{n}\in Z^D\setminus 0}\ln I_{\mathbf{n}} + \ln I_0(0). \quad (60)$$

Now, let us consider an observable $O(\mathbf{R}_i,\mathbf{P}_i)$ and its average,

$$\bar O = \frac{\int d\mathbf{P}_i d\mathbf{R}_i\, O(\mathbf{R}_i,\mathbf{P}_i)\exp(-\beta H_{\rm eff})}{\int d\mathbf{P}_i d\mathbf{R}_i \exp(-\beta H_{\rm eff})}. \quad (61)$$

We can use (60) to approximate $H_{\rm eff}$, namely

$$H_{\rm eff} \approx H_{RR} + \Phi - \frac{1}{\beta}\sum_{\mathbf{n}\in Z^D\setminus 0}\ln I_{\mathbf{n}} - \frac{1}{\beta}\ln I_0(0). \quad (62)$$

From (34) it follows that $I_{\mathbf{n}}$ is independent from $\mathbf{R}_i$ for the properly shifted integration variable. Applying (62) to (61), one can see that

$$\bar O = \frac{\int d\mathbf{P}_i d\mathbf{R}_i\, O(\mathbf{R}_i,\mathbf{P}_i)\exp[-\beta(H_{RR}+\Phi)]}{\int d\mathbf{P}_i d\mathbf{R}_i \exp[-\beta(H_{RR}+\Phi)]}, \quad (63)$$

which is independent from divergent $I_{\mathbf{n}}$. This reasoning, although not very rigorous, suggests that Φ and $U_{\rm eff}(\mathbf{R}_i-\mathbf{R}_j)$ might work for potentials with partially negative $\mathcal{V}(\mathbf{k})$ and can be useful in determining the mean values.

Finally, there are several concerns related to Φ itself. One thing is that we resort to the continuous representation of discrete expressions, though we expect Ω to be finite. This is physically reasonable provided that the range of microscopic potentials is much smaller than the system size L. Another issue is that we require microscopic potentials $V(r)$ and $U(r)$ to possess their Fourier transforms. This rules out such useful potentials as Lennard-Jones or polynomial potentials. Moreover, since (41) has the form of an inverse Fourier transform, the integrand must be "well-behaving," i.e., convergent for $k \to +\infty$ and without any essential singularities. Although in particular situations certain mathematical tricks and approximations can be applied to circumvent such problems, these are the reasons why (41) is not a directly applicable "silver bullet" formula.

III. APPLICATIONS

A. Systems under scrutiny

In this section, we apply $U_{\rm eff}(\mathbf{R}_i-\mathbf{R}_j)$ given by (41) to analyze effective interactions in various systems. First, we analyze the mixtures of Gaussian particles, predicting effective interactions and analyzing effective attraction as a driving force behind demixing (Sec. III B). Another example are screening effects in the system of charged hard spheres and ions which agree with the Derjaguin-Landau-Verwey-Overbeek (DLVO) potential (Sec. III C). Yet another example is the effective interaction in a binary mixture of Yukawa particles (Sec. III D). Finally, we scrutinize the mixture of particles that have both a Yukawa interaction tail and a repulsive core, in which case we qualitatively reproduce the effects of "attraction-through-repulsion"/"repulsion-through-attraction" and compare our results to simulations (Sec. III E).

B. Gaussian particles and demixing of binary mixtures

Particles interacting via the Gaussian potential are a typical example of soft particles, and they can be analyzed within our framework. We will take advantage of the fact that the Fourier transform of the Gaussian potential is also a Gaussian function:

$$G(r) = \epsilon e^{-\frac{1}{2}\frac{r^2}{\sigma^2}}, \quad \mathcal{G}(k) = \epsilon(2\pi)^{D/2}\sigma^D e^{-\frac{1}{2}k^2\sigma^2}. \tag{64}$$

The Gaussian potential has been identified as the accurate approximation of the interaction between two isolated polymers in a good solvent, both for identical [24] and nonidentical [36] chains. Therefore, the Gaussian-core model is a well established coarse-grained description of polymer solutions [1] both in the homogeneous and the nonhomogeneous case [37]. In particular, it has been found that the binary mixtures of Gaussian particles can undergo size separation transition [37,38], similarly to polymer blends.

In our model, we assume the binary mixture of different-sized Gaussian particles and assign index 1 to big-small interaction and 2 to small-small interaction. Then, the effective interaction, according to (41), reads

$$\begin{aligned} U_{\text{eff}}(\Delta R) &= -\frac{1}{(2\pi)^D}\int_{\tilde{\Omega}} d\mathbf{k}\, e^{i\mathbf{k}\cdot\Delta\mathbf{R}}\frac{|\mathcal{G}_1(k)|^2}{\mathcal{G}_2(k)} \\ &= -\frac{\epsilon_1^2}{\epsilon_2}\frac{\sigma_1^{2D}}{(2\pi)^{D/2}\sigma_2^D}\frac{e^{-\Delta R^2/(4\sigma_1^2-2\sigma_2^2)}}{\left(2\sigma_1^2-\sigma_2^2\right)^{D/2}}. \end{aligned} \tag{65}$$

$U_{\text{eff}}(\Delta R)$ proves to be a renormalized Gaussian, but, since $\epsilon_i > 0$, it is always negative. Examples of this interaction are presented in Fig. 1.

Result (65) suggests that the total interaction between bigger particles [i.e., $U_{RR}(\Delta R) + U_{\text{eff}}(\Delta R)$] can include an attractive tail, provided that for a certain choice of parameters there exist such ΔR that the effective interaction prevails over $U_{RR}(\Delta R)$. It is possible that such a tail could drive the separation process. Let the interaction between bigger particles read

$$U_{RR}(\Delta R) = G_0(\Delta R) = \epsilon_0 e^{-\frac{1}{2}\frac{\Delta R^2}{\sigma_0^2}}. \tag{66}$$

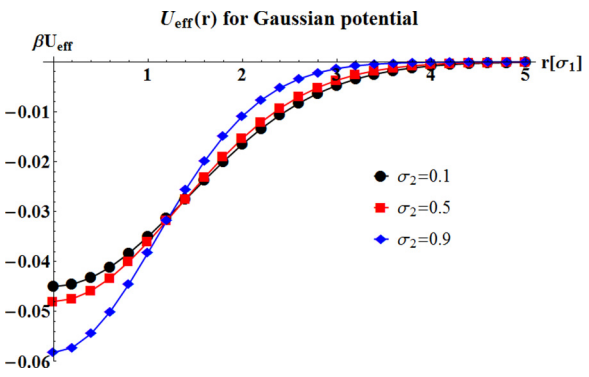

FIG. 1. (Color online) Effective interaction between Gaussian particles, according to formula (65). σ_1 is the unit length, and the scaling reads $\beta\epsilon_1^2/\epsilon_2 = 1$. U_{eff} is a negative Gaussian function for every σ_2.

The attractive tail will be present if the following inequality has a solution in ΔR:

$$G_0(\Delta R) + U_{\text{eff}}(\Delta R) < 0, \tag{67}$$

which can be reduced to

$$\begin{aligned} &\Delta R^2\left(\frac{1}{4\sigma_1^2-2\sigma_2^2}-\frac{1}{2\sigma_0^2}\right) \\ &< \ln\left(\frac{\epsilon_1^2}{\epsilon_0\epsilon_2}\frac{\sigma_1^{2D}}{(2\pi)^{D/2}\sigma_2^D}\frac{1}{\left(2\sigma_1^2-\sigma_2^2\right)^{D/2}}\right). \end{aligned} \tag{68}$$

This relation can be simplified further by assuming that $\sigma_1^2 = (\sigma_0^2+\sigma_2^2)/2$ and $\sigma_2 = c\sigma_0$, where c is the proportionality constant. Under such a choice of parameters, the right-hand side of (68) becomes identically 0, so the inequality reads

$$0 < \ln\left(\tilde{\epsilon}^2\frac{(1+c^2)^D}{(2\pi)^{D/2}c^D}\right), \tag{69}$$

where $\tilde{\epsilon} = \epsilon_1/\sqrt{\epsilon_0\epsilon_2}$ is a common energy scale. In Fig. 2, we have presented a region on the $\tilde{\epsilon}$-c plane where (69) is satisfied for $D = 3$. For comparison, in Fig. 2 we also plot the classical mean-field condition for spinodal separation of Gaussian particles, which reads [37,38]

$$\tilde{\epsilon} > \left(\frac{2c}{1+c^2}\right)^{3/2}. \tag{70}$$

Figure 2 illustrates a general qualitative agreement between the mean-field condition (70) and our condition (69), especially in terms of shape and the asymptotic behavior ($c \to 0$ and $c \gg 1$) of the mixing region. However, our

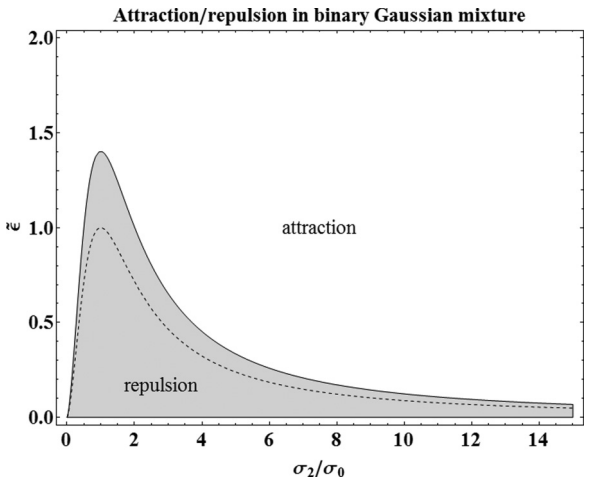

FIG. 2. Effective attraction in binary mixtures of Gaussian particles as a driving force behind phase separation. This plot visualizes inequality (69) for $D = 3$, where $\tilde{\epsilon} = \epsilon_1/\sqrt{\epsilon_0\epsilon_2}$ and $c = \sigma_2/\sigma_0$. Shaded region—total interaction is purely repulsive, no driving force for de-mixing. Plain region—total interaction has an attractive tail stimulating demixing. The dashed line illustrates mean-field condition (70) for spinodal decomposition in the Gaussian mixture.

theory systematically overshoots the mean-field behavior, with the highest discrepancy at $c \approx 1$. This means that the condition of attractive tail in total interaction leads to a broader region of mixing than the mean-field approach, which requires a higher sized ratio c or energy scale $\tilde{\epsilon}$ to obtain the separation.

C. Coulomb potential and charged sphere screening effects

In this example, we will examine the effective interaction between two charged hard spheres in the presence of ions. The dimensionality of the system is $D = 3$. Assigning index $i = 1$ for sphere-ion interaction and $i = 2$ for ion-ion interaction, we assume that every microscopic potential in this system consists of the hard-sphere (HS) potential and the Coulomb long-range interaction:

$$U_i(r) = U_{\mathrm{HS},i}(r) + V_{C,i}(r), \tag{71}$$

where

$$U_{\mathrm{HS},i}(r) = c_i \Theta(r - 2\sigma_i), \quad V_{C,i}(r) = \frac{\epsilon_i}{r}. \tag{72}$$

$\Theta(r - 2\sigma_i)$ is the Heaviside step function, the radius of the sphere reads σ_0, the ionic radius is denoted by σ_2 and $\sigma_1 = (\sigma_0 + \sigma_2)/2$, and c_i and ϵ_i are scaling constants.

The Fourier transform of the Coulomb potential can be calculated from its relation to the Yukawa potential:

$$V_{C,i}(r) = \frac{\epsilon_i}{r} = \lim_{\lambda \to 0} \frac{\epsilon_i e^{-\lambda r}}{r}. \tag{73}$$

Since the Fourier transform of the Yukawa potential is $4\pi/(k^2 + \lambda^2)$, then the sought-after Fourier transform reads

$$\mathcal{V}_{C,i}(k) = \frac{4\pi\epsilon_i}{k^2}. \tag{74}$$

The Fourier transform of $U_{\mathrm{HS},i}(r)$ can be calculated directly,

$$\mathcal{U}_{\mathrm{HS},i}(k) = 4\pi c_i \frac{\sin 2\sigma_i k - 2\sigma_i k \cos 2\sigma_i k}{k^3}. \tag{75}$$

This representation is adequate for sphere-ion interaction, but for ion-ion interaction we can simplify it significantly. Since σ_2 is the lowest length scale in the system, only k up to the order of $1/\sigma_2$ carries physically important information. In this range, we can approximate $\sin 2k\sigma_2 \simeq 2k\sigma_2$ and $\cos 2k\sigma_2 \simeq 1 - 2k^2\sigma_2^2$, so

$$\mathcal{U}_{\mathrm{HS},2}(k) \simeq 16\pi c_2 \sigma_2^3. \tag{76}$$

We would obtain a similar result by modeling the ion core with the Dirac-$\delta(\mathbf{r})$ potential, which indicates that (76) is, in fact, the pointlike approximation of $U_{\mathrm{HS},2}(r)$.

Having established both transforms, (41) can be applied and, after careful calculations, we obtain

$$\begin{aligned} U_{\mathrm{eff}}(\Delta R) &= -\frac{1}{(2\pi)^3} \int_{\tilde{\Omega}} d\mathbf{k}\, e^{i\mathbf{k}\cdot\Delta\mathbf{R}} \frac{|\mathcal{U}_{\mathrm{HS},1}(k) + \mathcal{V}_{C,1}(k)|^2}{\mathcal{U}_{\mathrm{HS},2}(k) + \mathcal{V}_{C,2}(k)} \\ &= -\frac{\epsilon_1^2}{\epsilon_2} \frac{1}{\Delta R} + C_0 \frac{e^{-\frac{\kappa_{\mathrm{eff}}}{2}\Delta R}}{\Delta R}. \end{aligned} \tag{77}$$

This result consists of Coulomb-like and Yukawa-like terms, and it is valid for $\Delta R > 4\sigma_1$. The constants read

$$\kappa_{\mathrm{eff}} = \sqrt{\frac{\epsilon_2}{c_2\sigma_2^3}}, \tag{78}$$

$$C_0 = \frac{c_2\sigma_2^3}{\epsilon_2^2}(\epsilon_1\kappa_{\mathrm{eff}} - 2c_1\sigma_1\kappa_{\mathrm{eff}} \cosh\sigma_1\kappa_{\mathrm{eff}} + 2c_1 \sinh\sigma_1\kappa_{\mathrm{eff}})^2. \tag{79}$$

Let us further specify our system by assuming that the charge of a single sphere reads Q and the charge of an ion is q. Then

$$\epsilon_1 = \frac{qQ}{4\pi\varepsilon}, \quad \epsilon_2 = \frac{q^2}{4\pi\varepsilon}, \quad \frac{\epsilon_1^2}{\epsilon_2} = \frac{Q^2}{4\pi\varepsilon}, \tag{80}$$

where ε is the electrostatic permittivity of the system. Since all spheres have the same charge, there is also a microscopic repulsion present, which, for $\Delta R \gg 2\sigma_0$, can be treated as a Coulomb potential:

$$U_{RR}(\Delta R) = \frac{Q^2}{4\pi\varepsilon\Delta R}. \tag{81}$$

Calculating the total sphere-sphere interaction, we obtain

$$U_{\mathrm{tot}}(\Delta R) = U_{RR}(\Delta R) + U_{\mathrm{eff}}(\Delta R) = C_0 \frac{e^{-\frac{\kappa_{\mathrm{eff}}}{2}\Delta R}}{\Delta R}. \tag{82}$$

One can immediately see that the Coulomb term from (77) cancels the long-range repulsion $U_{RR}(\Delta R)$, thus the total interaction consists solely of the Yukawa term. This term has the same functional form as the DLVO potential [9] in the Debye-Hückel (DH) approximation, which reads [22,39]

$$U_{\mathrm{DLVO}}(\Delta R) = C_{\mathrm{DLVO}} \frac{e^{-\kappa_{\mathrm{DH}}\Delta R}}{\Delta R}, \tag{83}$$

where

$$\kappa_{\mathrm{DH}}^2 = \beta\frac{4\pi}{\varepsilon}(n_1 Q^2 + n_2 q^2), \quad C_{\mathrm{DLVO}} = \frac{Q^2 e^{2\sigma_0\kappa_{\mathrm{DH}}}}{\varepsilon(1 + 2\sigma_0\kappa_{\mathrm{DH}})^2},$$

with n_1, n_2 the number densities of spheres and ions, respectively.

In our model, we expect that $c_i \gg k_B T$, so $U_{\mathrm{HS},i}(r)$ acts as an impenetrable core, but these core constants are not defined otherwise. However, by comparing (82) and (83),

$$\begin{aligned} 2\kappa_{\mathrm{DH}} &= \kappa_{\mathrm{eff}}, \\ C_0 &= C_{\mathrm{DLVO}}, \end{aligned} \tag{84}$$

we can relate c_i to the DLVO parameters:

$$\begin{aligned} c_2 &= \frac{\epsilon_2}{4\kappa_{\mathrm{DH}}^2\sigma_2^3}, \\ c_1 &= \frac{\kappa_{\mathrm{DH}}(\epsilon_1 \pm \sqrt{\epsilon_2|C_{\mathrm{DLVO}}|})}{2\sigma_1\kappa_{\mathrm{DH}}\cosh 2\sigma_1\kappa_{\mathrm{DH}} - \sinh 2\sigma_1\kappa_{\mathrm{DH}}}, \end{aligned} \tag{85}$$

where the sign is chosen so $c_1 > 0$. This choice of c_1 and c_2 tunes (82) to become exactly the DLVO interaction (83). In [22], Crocker and Grier have measured $\kappa_{\mathrm{DH}}^{-1} = 161$ nm for polystyrene sulfate spheres of radius $\sigma_0 = 32$ nm and charge $Q = 1991\mathrm{e}$. Assuming $\sigma_2 = 0.1$ nm and $q = -\mathrm{e}$, one can

calculate that $\beta c_1 \simeq 13$ and $\beta c_2 \simeq 10^{13}$ for $T = 298$ K. This is in agreement with our expectation that $c_i \gg k_B T$.

In conclusion, our model based on the formula (41) proves to be equivalent to the DLVO potential, which has been shown to accurately describe screening effects for the charged spheres in colloidal solution [22].

D. Yukawa particles

As discussed in the preceding section, the Yukawa potential is an accurate model for charged particles in solution. Since this potential is also tractable in terms of its Fourier transform, analyzing the binary mixture of Yukawa particles is another interesting example for our theory. For $D = 3$, the Yukawa potential $Y(r)$ and its Fourier transform read

$$Y(r) = \epsilon\sigma \frac{e^{-\kappa(r-\sigma)}}{r}, \quad \mathcal{Y}(k) = \frac{4\pi\epsilon\sigma e^{\kappa\sigma}}{k^2+\kappa^2}. \tag{86}$$

Let us consider a system composed of Yukawa particles, where $\sigma_1, \epsilon_1, \kappa_1$ describe particle-depletant interaction $Y_1(r)$, and depletant-depletant interaction $Y_2(r)$ depends on $\sigma_2, \epsilon_2, \kappa_2$. Then, the effective interaction can be calculated analytically from (41), namely

$$\begin{aligned} U_{\text{eff}}(\Delta R) &= -\frac{1}{(2\pi)^3}\int_{\tilde{\Omega}} d\mathbf{k}\, e^{i\mathbf{k}\cdot\Delta\mathbf{R}} \frac{|\mathcal{Y}_1(k)|^2}{\mathcal{Y}_2(k)} \\ &= -\frac{\epsilon_1^2\sigma_1^2}{\epsilon_2\sigma_2} e^{-\kappa_1(\Delta R - 2\sigma_1)-\kappa_2\sigma_2}\left(\frac{1}{\Delta R} - \frac{\kappa_1^2-\kappa_2^2}{2\kappa_1}\right). \end{aligned} \tag{87}$$

A graphical representation of (87) for various parameters is shown in Fig. 3. In general, for $\epsilon_2 > 0$ the particular profiles of effective interaction are strongly dependent on parameters and can vary from purely attractive to strongly repulsive. When the range of interaction is of the order of particle radius ($\kappa_i \simeq \sigma_i^{-1}$), the effective interaction is attractive (curves 1–3 in Fig. 3) and its range increases with the downturn in the depletant radius. In fact, this range is surprisingly long, namely for $\sigma_2/\sigma_1 = 0.25$ the interaction is significant over a range of $5\sigma_1$ (curve 1, Fig. 3). This is in stark contrast with the

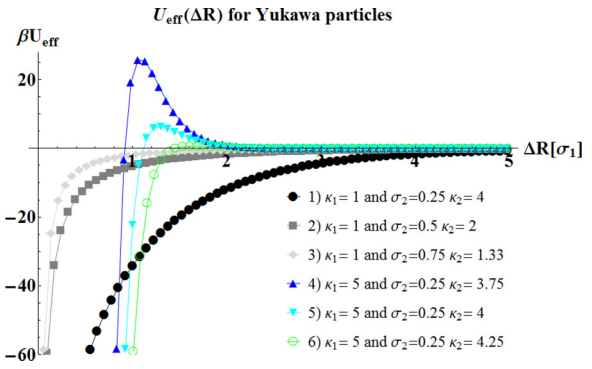

FIG. 3. (Color online) Effective potential for a binary mixture of Yukawa particles, according to formula (87), for which $\beta\epsilon_1^2/\epsilon_2 = 1$, and σ_2 and κ_i are given in units $[\sigma_1]$ and $[\sigma_1^{-1}]$, respectively. Curves 1–3: growing depletion attraction for decreasing size of depletant particles, $\kappa_i = \sigma_i^{-1}$, to match the size of the particle. Curves 4–6: for higher values of κ_1, a κ_2-dependent energy barrier appears.

Asakura-Oosawa model for HS of radii σ_1 and σ_2, where the interaction would cease over a range of $\sigma_1 + \sigma_2$ [16]. Another interesting characteristic of U_{eff} for Yukawa particles appears when κ_1 is increased, in which case a repulsive barrier emerges. This barrier grows as the range of depletant-depletant interaction increases (curves 4–6, Fig. 3). Apparently, possible energetic advantages of lower $Y_1(r)$ cannot dominate the depletant-depletant repulsion. Finally, if we assume $\epsilon_2 < 0$, the global sign of $U_{\text{eff}}(\Delta R)$ is inversed, leading to repulsion-through-attraction effects.

Summarizing, this relatively simple model indicates possible self-organization of Yukawa particles, although analytical calculations analogous to Gaussian particles cannot be easily completed here. Nevertheless, phase separation in binary Yukawa systems has been encountered in simulations [41] and also in the context of plasma research, e.g., [42,43].

E. Particles with a repulsive core and a Yukawa interaction tail

The pure Yukawa potential suffers from the lack of a repulsive core independent from the interaction tail, so a realistic description of colloid particles requires a more complicated potential. In [25], Louis *et al.* simulated a binary system consisting of HS particles with Yukawa interaction tails, both as depletant and colloid particles. The potential applied in [25] reads

$$\begin{cases} +\infty & \text{if} \quad r < \sigma_i, \\ \dfrac{\epsilon_i\sigma_i}{r} e^{-\kappa_i(r-\sigma_i)} & \text{if} \quad r \geqslant \sigma_i, \end{cases} \tag{88}$$

where index i denotes big-small or small-small potential, σ_i is the size of the particle core, and ϵ_i is the energy scale. Reference [25] reports that the sign of the big-small interaction tail is decisive for the effective interaction being attractive or repulsive. In particular, the repulsive tail results in effective attraction in the system, while the attractive tail induces "repulsion-through-attraction." Within our framework, we are able to qualitatively reproduce these two effects with an analytical formula.

We propose to model both the hard core and interaction tail of a single particle with two Yukawa potentials, namely

$$Y_i^{\text{HS}}(r) = \frac{c_i\sigma_i}{r} e^{-\lambda_i(r-\sigma_i)} + \frac{t_i\sigma_i}{r} e^{-\kappa_i(r-\sigma_i)}, \tag{89}$$

where index $i = 1$ denotes particle-depletant interaction and $i = 2$ denotes depletant-depletant interaction. For $\lambda_i > \kappa_i$, the first term becomes a repulsive core, while the second term can now be either repulsive or attractive, depending on t_i. To allow a direct comparison between our results and [25], we would like to control the attractive tail of $Y_i^{\text{HS}}(r)$ with the depth of its minimum ϵ_i. Thus, for $\epsilon_i < 0$ we have determined t_i numerically from the following equations:

$$\begin{aligned} \tfrac{d}{dr} Y_i^{\text{HS}}(r)\big|_{r=r_0} &= 0, \\ Y_i^{\text{HS}}(r_0) &= \epsilon_i. \end{aligned} \tag{90}$$

In the case of a repulsive tail, we have assumed $t_i = \epsilon_i \geqslant 0$.

The Fourier transform of $Y_i^{\text{HS}}(r)$ is simply a sum of two $\mathcal{Y}(k)$ for relevant parameters. Therefore, the effective interaction

reads

$$U_{\text{eff}}(\Delta R) = -\frac{1}{(2\pi)^3}\int_{\tilde{\Omega}} d\mathbf{k}\, e^{i\mathbf{k}\cdot\Delta\mathbf{R}}\frac{|\mathcal{Y}_1^{\text{HS}}(k)|^2}{\mathcal{Y}_2^{\text{HS}}(k)}$$
$$= -\frac{2}{\pi}\frac{\sigma_1^2}{\sigma_2}\int_0^{+\infty} dk \frac{k\sin\Delta Rk}{\Delta R}\frac{\left(k^2+\kappa_2^2\right)\left(k^2+\lambda_2^2\right)}{\left(k^2+\lambda_1^2\right)^2\left(k^2+\kappa_1^2\right)^2}$$
$$\times\frac{\left[c_1 e^{\sigma_1\lambda_1}\left(k^2+\kappa_1^2\right)+t_1 e^{\kappa_1\sigma_1}\left(k^2+\lambda_1^2\right)\right]^2}{\left[c_2 e^{\sigma_2\lambda_2}\left(k^2+\kappa_2^2\right)+t_2 e^{\kappa_2\sigma_2}\left(k^2+\lambda_2^2\right)\right]}. \quad (91)$$

The integrand in the above expression is an even function, and the degree of polynomial expression in the denominator is higher than that in the numerator, so this integral can be calculated analytically, thanks to the residue theorem. Due to its length and complexity, we discuss the full formula in the Appendix.

The core parameters c_i and λ_i cannot be determined from first principles, and our initial experience with (91) has shown that the exact shape of interactions obtained from our model is very sensitive to these parameters. It is also usually possible to find the parameters that differ by many orders of magnitude but lead to similar results. Therefore, in order to determine the physically reasonable range of core parameters, we have fitted our model to the simulation data from [25]. In [25], the values of potential parameters read $\sigma_1 = 0.6\sigma_0$, $\sigma_2 = 0.2\sigma_0$, $\kappa_1 = 6/\sigma_0$, and $\kappa_2 = 15/\sigma_0$, where σ_0 is the radius of the bigger particle. The simulations have been performed for nine combinations of tail parameters, namely for $\beta\epsilon_1$ equal to -0.82, 0, and 0.82, and for $\beta\epsilon_2$ set to 0, 2.99, and -0.996. We read the data from Fig. 6 in [25] with the resolution of 25 points per curve and fit them using the quasi-Newton algorithm with a constraint $c_i > 0$. The constraint is applied to prevent the tendency of the algorithm to find the unphysical values of parameters.

To fit the data, we should find four core parameters c_i and λ_i for each choice of ϵ_1 and ϵ_2. However, the algorithm usually could not achieve convergence if λ_1 and λ_2 have been varied. Therefore, we have chosen $\lambda_1 = 3\kappa_1$ and $\lambda_2 = 2.4\kappa_2$ and kept these values constant for all curves, fitting solely c_1 and c_2. For such a choice of λ_i, the microscopic potentials $Y_i^{\text{HS}}(\Delta R)$ are relatively soft-core, but this choice improved the quality of fits for all $\epsilon_2 \neq 0$ cases, with the error of c_1 up to 15% (except for case 3, which was 44%) and the errors of c_2 lower than 0.0002%. However, extreme errors (higher than 500%) are encountered for all $\epsilon_2 = 0$ cases (plots 1, 4, and 7, Fig. 4), though the algorithm achieved convergence even in this situation. These errors might arise from the fact that we fit the

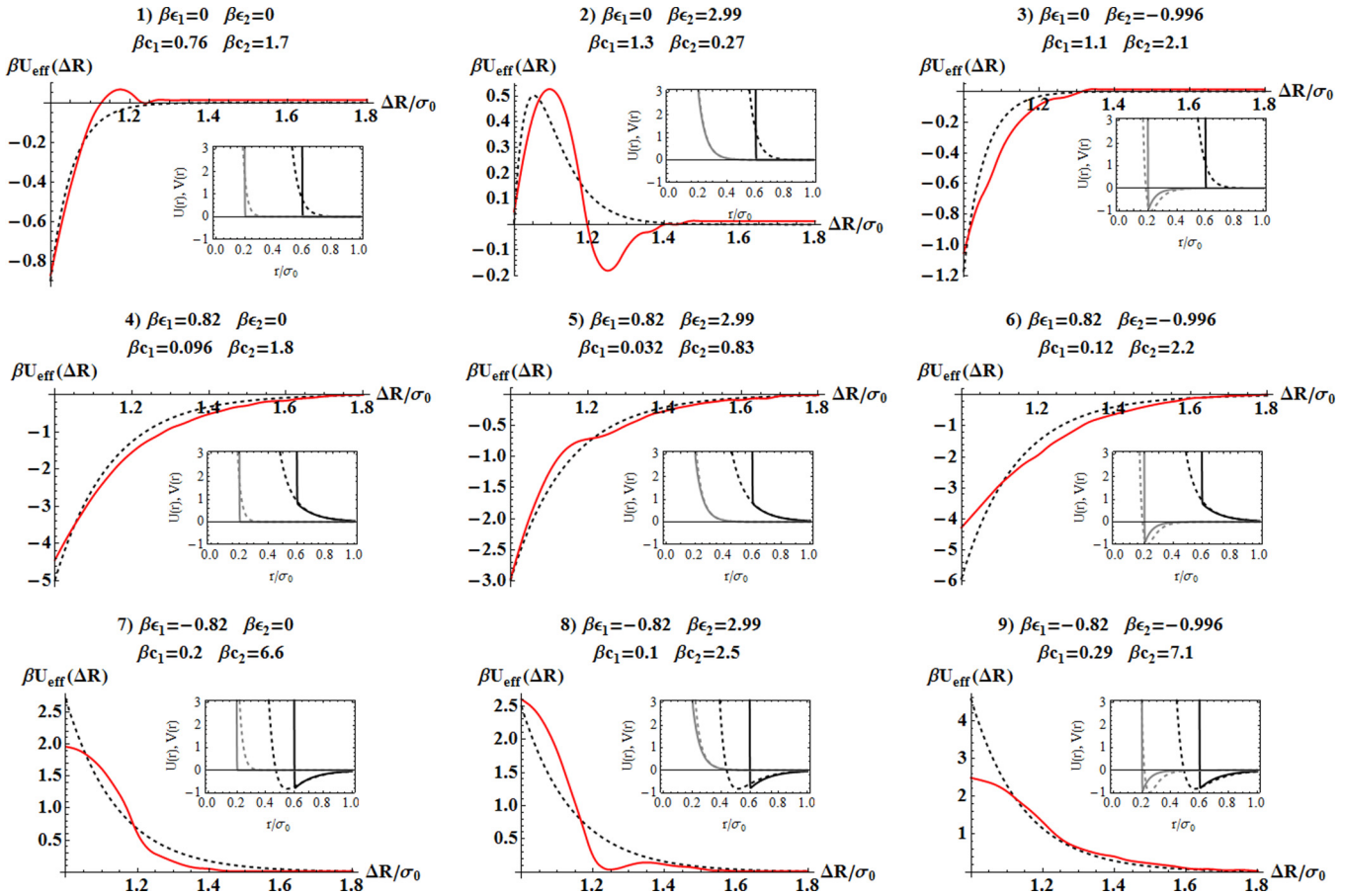

FIG. 4. (Color online) Model (91) (dashed black line) fitted to simulation data (red solid line) from [25]. In all cases, core exponents read $\lambda_1 = 3\kappa_1$ and $\lambda_2 = 2.4\kappa_2$; c_i are determined from the fitting procedure. Insets: a comparison between potential wells resulting from the fitting procedure and the hard-core potentials applied in [25]; gray, small-small interaction; black, big-small interaction; dashed lines, soft-core potential generated with λ_i and c_i; solid lines, referential hard-core potential from [25].

essentially soft-core model to the data that are directly affected by the hard-core potential. In the absence of mitigating effects from the tail, our model becomes highly sensitive to λ_i, though no such problem is encountered for $\epsilon_1 = 0$. While increasing λ_i might improve those three fits, we have decided to keep common λ_i for all examples, to allow as much comparison between them as possible.

The data from simulations and our fits are presented in Fig. 4. In general, our model is capable of reproducing all types of effective interactions found in [25] in terms of their sign and range. In particular, our model reproduces the "attraction-though-repulsion" effect for $\epsilon_1 > 0$ (plots 4–6, Fig. 4) and the "repulsion-through-attraction" effect for $\epsilon_1 < 0$ (plots 7–9, Fig. 4). In the former case, our model exhibits a general tendency to predict a shallower effective potential than in the simulations. However, in the latter case of $\epsilon_1 < 0$ our model evidently lacks the oscillatory behavior which is manifested in the simulations. This is also a problem for the $\epsilon_1 = 0$, $\epsilon_2 = 2.99$ case (plot 2, Fig. 4), which is entirely dominated by the oscillations, and, to a lesser extent, for the pure hard-sphere case ($\epsilon_1 = 0$, $\epsilon_2 = 0$, plot 1, Fig. 4). In all of these examples, our model can be applied only qualitatively, whenever the oscillations can be treated as a higher-order effect. In the insets of Fig. 4, there are also microscopic potential wells presented, generated according to fitted parameters, and compared to the HS potentials applied in the simulations. As expected, the highest discrepancies occur for $\epsilon_1 < 0$, most likely due to the lack of oscillations. The other examples show agreement in the shape of the interaction tail, though for $\epsilon_i = 0$ a compensating softening of the core occurs.

In principle, varying solely ϵ_1 and ϵ_2 should be enough to explain the differences in effective interaction for a common set of core parameters. Taking the suggestion from the previously fitted parameters, we have chosen $\lambda_1 = \frac{5}{3}\kappa_1$, $\lambda_2 = \frac{32}{15}\kappa_2$, $\beta c_1 = 1$, and $\beta c_2 = 2.2$. The results are shown in Fig. 5. For such a choice of parameters, the core part of the microscopic potential is even softer than before, but now our model simultaneously reproduces eight out of nine types of simulated effective interactions, in terms of their energy scale, range, and sign. As before, our predictions lack the oscillations for $\epsilon_1 < 0$, which is one group of results (curves 7–9, Fig. 5). In this case, our predictions might be treated only as a crude approximation. Another group is the effective attraction for $\epsilon_1 > 0$ (curves 4–6, Fig. 5). In this group, our predictions vary more uniformly with changing ϵ_2 than in the simulations, and our effective potential is usually stronger for $\Delta R/\sigma_0$ close to 1, but sooner becomes flat. Yet another group is formed by $\epsilon_1 = 0$ results. The sole qualitative disagreement occurs for the $\epsilon_1 = 0$, $\epsilon_2 = 2.99$ case (curve 2, Fig. 5), which is predicted as attractive, but the simulations show its mainly oscillatory behavior. In the remaining cases of $\epsilon_1 = 0$, $\epsilon_2 = 0$ and $\epsilon_1 = 0$, $\epsilon_2 = -0.996$ (curves 1 and 2, Fig. 5), the predicted range of interaction is slightly longer than in simulations.

In summary, (91) qualitatively reproduces most of the expected effective interaction characteristics. The discrepancies between our model and simulations might originate from both the application of soft-core potentials and the fact that Φ is only a part of the total effective interaction. In the Appendix, we comment briefly on the possibility of generating oscillatory behavior from (91).

IV. FINAL REMARKS

In this paper, we have proposed an occupation number functional as a tool to describe binary colloidal systems. This functional is an alternative to the Asakura-Oosawa approach, density functional theory, and closure relations. In Sec. III, we have shown that with the aid of our formalism, we are able to reproduce analytically the important features of systems ranging from Gaussian particle mixtures to Yukawa particle mixtures. Our theory proved to be a versatile qualitative tool, which supports our proposition that $U_{\text{eff}}(\mathbf{R}_i - \mathbf{R}_j)$ can be the dominant source of effective interactions. While the

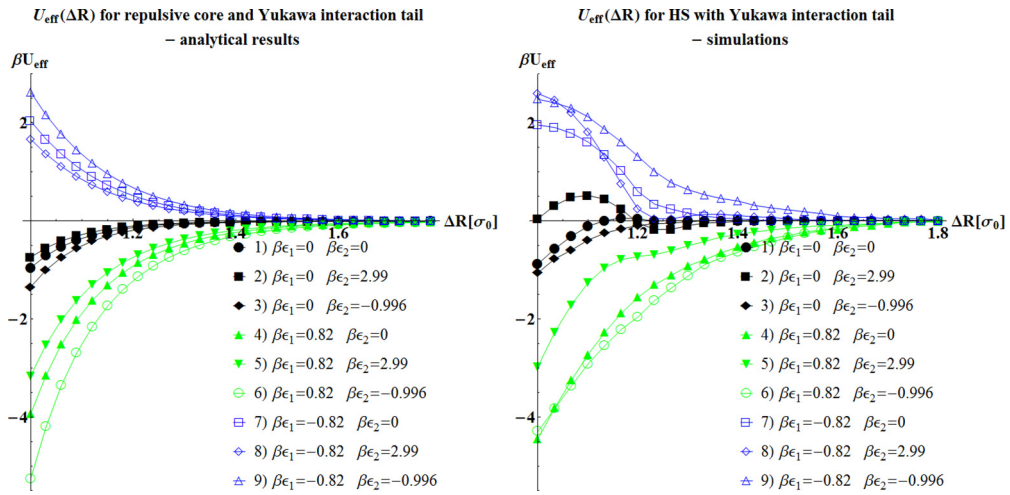

FIG. 5. (Color online) Effective interaction in the binary mixture of particles consisting of a repulsive core and a Yukawa interaction tail. Left: effective interaction generated from formula (91) for soft-core particles. Right: effective interaction measured in the simulations of hard-core particles, reprinted from [25]. σ_0 is the radius of bigger particles, $\sigma_1 = 0.6\sigma_0$, $\sigma_2 = 0.2\sigma_0$, $\kappa_1 = 6/\sigma_0$, and $\kappa_2 = 15/\sigma_0$. Core parameters for all curves: $\lambda_1 = \frac{5}{3}\kappa_1$, $\lambda_2 = \frac{32}{15}\kappa_2$, $\beta c_1 = 1$, and $\beta c_2 = 2.2$. Curves 1–3: for $\epsilon_1 = 0$, the behavior of U_{eff} depends on the sign of ϵ_2. Curves 4–6: for $\epsilon_1 > 0$, U_{eff} is attractive. Curves 7–9: for $\epsilon_1 < 0$, U_{eff} is repulsive.

framework we propose is currently far less developed and not as accurate as other approaches in the field, it provides a more direct insight into how effective interactions arise from microscopic potentials. We have provided a discussion on the assumptions and approximations that determine the limits of applicability for our theory. Further development of the occupation number functional approach might include reproducing thermodynamics of binary systems or relating this model to spatiotemporal correlations in noise in a Langevin-like description.

ACKNOWLEDGMENTS

M.M. acknowledges the support of the M. Smoluchowski KRAKOW SCIENTIFIC CONSORTIUM, in the framework of the KNOW scholarship.

APPENDIX: FULL FORMULA FOR THE EFFECTIVE INTERACTION OF PARTICLES WITH A REPULSIVE CORE AND A YUKAWA INTERACTION TAIL

In this appendix, we present the full analytic formula for effective interaction given by (91):

$$\begin{aligned} U_{\text{eff}}(\Delta R) &= -\frac{1}{(2\pi)^3}\int_{\tilde{\Omega}} d\mathbf{k}\, e^{i\mathbf{k}\cdot\Delta\mathbf{R}}\frac{\left|\mathcal{Y}_1^{\text{HS}}(k)\right|^2}{\mathcal{Y}_2^{\text{HS}}(k)} \\ &= -\frac{2}{\pi}\frac{\sigma_1^2}{\sigma_2}\int_0^{+\infty} dk\frac{k\sin\Delta Rk}{\Delta R}\frac{\left(k^2+\kappa_2^2\right)\left(k^2+\lambda_2^2\right)}{\left(k^2+\lambda_1^2\right)^2\left(k^2+\kappa_1^2\right)^2}\frac{\left[c_1e^{\sigma_1\lambda_1}\left(k^2+\kappa_1^2\right)+t_1e^{\kappa_1\sigma_1}\left(k^2+\lambda_1^2\right)\right]^2}{\left[c_2e^{\sigma_2\lambda_2}\left(k^2+\kappa_2^2\right)+t_2e^{\kappa_2\sigma_2}\left(k^2+\lambda_2^2\right)\right].} \end{aligned} \tag{A1}$$

The integrand is the even function of k, and the nominator has lower order than the denominator, so this integral can be calculated via residue theorem. The integrand has four poles:

$$k_1 = i\lambda_1, \tag{A2}$$

$$k_2 = i\kappa_1, \tag{A3}$$

$$k_{3,\pm} = \pm i\sqrt{\frac{c_2\kappa_2^2e^{\sigma_2\lambda_2}+t_2\lambda_2^2e^{\sigma_2\kappa_2}}{c_2e^{\lambda_2\sigma_2}+t_2e^{\kappa_2\sigma_2}}}. \tag{A4}$$

k_1 and k_2 lie in the upper complex half-plane. $k_{3,\pm}$ can be either purely imaginary, in which case only $k_{3,+}$ lies in the upper complex half-plane, or purely real, in which case both $k_{3,+}$ and $k_{3,-}$ lie on the real axis. For three imaginary poles, the result of integration reads

$$U_{\text{eff}}(\Delta R) = 2\pi i[\text{Res}(k_1)+\text{Res}(k_2)+\text{Res}(k_{3,+})], \tag{A5}$$

where

$$\begin{aligned} 2\pi i\,\text{Res}(k_1) = \frac{\sigma_1^2}{\sigma_2}c_1e^{\lambda_1(\sigma_1-\Delta R)}\{&4t_1\lambda_1e^{\kappa_1\sigma_1}\left(\kappa_2^2-\lambda_1^2\right)\left(\lambda_2^2-\lambda_1^2\right)\left[c_2e^{\lambda_2\sigma_2}\left(\kappa_2^2-\lambda_1^2\right)-t_2e^{\kappa_2\sigma_2}\left(\lambda_1^2-\lambda_2^2\right)\right] \\ &-c_1e^{\lambda_1\sigma_1}\left(\kappa_1^2-\lambda_1^2\right)\left[t_2e^{\kappa_2\sigma_2}\left[\Delta R\left(\lambda_1^2-\kappa_2^2\right)-2\lambda_1\right]\left(\lambda_1^2-\lambda_2^2\right)^2+c_2e^{\lambda_2\sigma_2}\left(\kappa_2^2-\lambda_1^2\right)^2\left[\Delta R\left(\lambda_1^2-\lambda_2^2\right)-2\lambda_1\right]\right]\} \\ &/\left\{\lambda_1\Delta R\left(\lambda_1^2-\kappa_1^2\right)\left[c_2e^{\lambda_2\sigma_2}\left(\kappa_2^2-\lambda_1^2\right)-t_2e^{\kappa_2\sigma_2}\left(\lambda_1^2-\lambda_2^2\right)\right]^2\right\}, \end{aligned} \tag{A6}$$

$$\begin{aligned} 2\pi i\,\text{Res}(k_2) = \frac{\sigma_1^2}{\sigma_2}t_1e^{\kappa_1(\sigma_1-\Delta R)}\{&4c_1\kappa_1e^{\lambda_1\sigma_1}\left(\kappa_1^2-\kappa_2^2\right)\left(\lambda_2^2-\kappa_1^2\right)\left[c_2e^{\lambda_2\sigma_2}\left(\kappa_1^2-\kappa_2^2\right)+t_2e^{\kappa_2\sigma_2}\left(\kappa_1^2-\lambda_2^2\right)\right] \\ &+t_1e^{\kappa_1\sigma_1}\left(\kappa_1^2-\lambda_1^2\right)\left[t_2e^{\kappa_2\sigma_2}\left(\kappa_1^2-\lambda_2^2\right)^2\left[\Delta R\left(\kappa_1^2-\kappa_2^2\right)-2\kappa_1\right]+c_2e^{\lambda_2\sigma_2}\left(\kappa_1^2-\kappa_2^2\right)^2\left[\Delta R\left(\kappa_1^2-\lambda_2^2\right)-2\kappa_1\right]\right]\} \\ &/\left\{\kappa_1\Delta R\left(\kappa_1^2-\lambda_1^2\right)\left[c_2e^{\lambda_2\sigma_2}\left(\kappa_1^2-\kappa_2^2\right)+t_2e^{\kappa_2\sigma_2}\left(\kappa_1^2-\lambda_2^2\right)\right]^2\right\}, \end{aligned} \tag{A7}$$

$$\begin{aligned} 2\pi\, i\text{Res}(k_{3,+}) = 2\frac{\sigma_1^2}{\sigma_2}c_2t_2\left(\kappa_2^2-\lambda_2^2\right)^2\exp&\left(\sigma_2(\kappa_2+\lambda_2)-\Delta R\sqrt{\frac{c_2\kappa_2^2e^{\lambda_2\sigma_2}+t_2\lambda_2^2e^{\kappa_2\sigma_2}}{c_2e^{\lambda_2\sigma_2}+t_2e^{\kappa_2\sigma_2}}}\right) \\ &\times\left\{c_1e^{\lambda_1\sigma_1}\left[c_2e^{\lambda_2\sigma_2}\left(\kappa_1^2-\kappa_2^2\right)+t_2e^{\kappa_2\sigma_2}\left(\kappa_1^2-\lambda_2^2\right)\right]-t_1e^{\kappa_1\sigma_1}\left[c_2e^{\lambda_2\sigma_2}\left(\kappa_2^2-\lambda_1^2\right)-t_2e^{\kappa_2\sigma_2}\left(\lambda_1^2-\lambda_2^2\right)\right]\right\}^2 \\ &/\left\{\Delta R\left(c_2e^{\lambda_2\sigma_2}+t_2e^{\kappa_2\sigma_2}\right)\left[c_2e^{\lambda_2\sigma_2}\left(\kappa_1^2-\kappa_2^2\right)+t_2e^{\kappa_2\sigma_2}\left(\kappa_1^2-\lambda_2^2\right)\right]^2\left[c_2e^{\lambda_2\sigma_2}\left(\kappa_2^2-\lambda_1^2\right)-t_2e^{\kappa_2\sigma_2}\left(\lambda_1^2-\lambda_2^2\right)\right]^2\right\}. \end{aligned} \tag{A8}$$

In the case of real $k_{3,\pm}$, the contribution $2\pi i\,\mathrm{Res}(k_{3,+})$ must be replaced with

$$\pi i[\mathrm{Res}(k_{3,+})+\mathrm{Res}(k_{3,-})]=4\frac{\sigma_1^2}{\sigma_2}c_2t_2\left(\kappa_2^2-\lambda_2^2\right)^2e^{\sigma_2(\kappa_2+\lambda_2)}\cos\left(\Delta R\sqrt{\left|\frac{c_2\kappa_2^2e^{\lambda_2\sigma_2}+t_2\lambda_2^2e^{\kappa_2\sigma_2}}{c_2e^{\lambda_2\sigma_2}+t_2e^{\kappa_2\sigma_2}}\right|}\right)$$
$$\times\left\{c_1e^{\lambda_1\sigma_1}\left[c_2e^{\lambda_2\sigma_2}\left(\kappa_1^2-\kappa_2^2\right)+t_2e^{\kappa_2\sigma_2}\left(\kappa_1^2-\lambda_2^2\right)\right]-t_1e^{\kappa_1\sigma_1}\left[c_2e^{\lambda_2\sigma_2}\left(\kappa_2^2-\lambda_1^2\right)-t_2e^{\kappa_2\sigma_2}\left(\lambda_1^2-\lambda_2^2\right)\right]\right\}^2$$
$$\Big/\left\{\Delta R\left(c_2e^{\lambda_2\sigma_2}+t_2e^{\kappa_2\sigma_2}\right)\left[c_2e^{\lambda_2\sigma_2}\left(\kappa_1^2-\kappa_2^2\right)+t_2e^{\kappa_2\sigma_2}\left(\kappa_1^2-\lambda_2^2\right)\right]^2\left[c_2e^{\lambda_2\sigma_2}\left(\kappa_2^2-\lambda_1^2\right)\right.\right.$$
$$\left.\left.-t_2e^{\kappa_2\sigma_2}\left(\lambda_1^2-\lambda_2^2\right)\right]^2\right\}. \tag{A9}$$

In general, the obtained formula for (A5) is a combination of Yukawa-like and exponential functions. Looking at the final expressions from the perspective of λ_1 and λ_2, one can see that there are several exponent terms that differ in their characteristic "length scale," some of them even divergent for growing λ_i. This explains the sensitivity of the model to core parameters, and it is probably the reason for the numerical difficulties encountered in the fitting procedure when λ_i are varied.

Interestingly, the contribution (A9) might introduce oscillatory behavior, which is apparently missing in Sec. III E. However, this contribution appears for $-\frac{\kappa_2^2}{\lambda_2^2}c_2e^{\sigma_2(\kappa_2-\lambda_2)}>t_2>-c_2e^{\sigma_2(\kappa_2-\lambda_2)}$, which means that t_2 must be negative. In our model, $t_2<0$ requires $\epsilon_2<0$ [by (90)], so only cases 3, 6, and 9 from Fig. 4 could be affected by oscillations from (A9). This means that in the discussed model, it is not possible to choose the core parameters that provide oscillations in cases 2, 7, and 8 from Fig. 4. Therefore, this effect is most likely embedded in the neglected part of the effective interaction.

[1] C. N. Likos, Phys. Rep. **348**, 267 (2001).
[2] A. Strander, H. Sedgwick, F. Cardinaux, W. C. K. Poon, S. U. Egelhaaf, and P. Schurtenberger, Nature (London) **432**, 492 (2004).
[3] E. R. Weeks, J. C. Crocker, and D. A. Weitz, J. Phys.: Condens. Matter **19**, 205131 (2007).
[4] D. Marenduzzo, K. Finan, and P. R. Cook, J. Cell. Biol. **175**, 5 (2006).
[5] H. Dietsch, V. Malik, M. Reufer, C. Dagallier, A. Shalkevich, M. Saric, T. Gibaud, F. Cardinaux, F. Scheffold, A. Stradner, and P. Schurtenberger, Chimia **62**, 805 (2008).
[6] A. Kudrolli, Rep. Prog. Phys. **67**, 209 (2004).
[7] S. Aumaitre, C. A. Kruelle, and I. Rehberg, Phys. Rev. E **64**, 041305 (2001).
[8] J. P. Hansen and I. R. McDonald, *Theory of Simple Liquids* (Elsevier Academic, London, 2006).
[9] H. N. W. Lekkerkerker and R. Tuinier, *Colloids and the Depletion Interaction* (Springer, London, 2011).
[10] S. Asakura and F. Oosawa, J. Polym. Sci. **33**, 183 (1958).
[11] S. Asakura and F. Oosawa, J. Chem. Phys. **22**, 1255 (1954).
[12] A. Vrij, Pure Appl. Chem. **48**, 471 (1976).
[13] K. Yaman, C. Jeppesen, and C. M. Marques, Europhys. Lett. **42**, 221 (1998).
[14] P. R. Lang, J. Chem. Phys. **127**, 124906 (2007).
[15] D. G. Grier, Nature (London) **424**, 810 (2003).
[16] A. G. Yodh, K. Lin, J. C. Crocker, A. D. Dinsmore, R. Verma, and P. D. Kaplan, Phil. Trans. R. Soc. Lond. A **359**, 921 (2001).
[17] E. Donth, H. Huth, and M. Beiner, J. Phys.: Condens. Matter **13**, L451 (2001).
[18] C. Dalle-Ferrier, C. Thibierge, C. Alba-Simionesco, L. Berthier, G. Biroli, J. P. Bouchaud, F. Ladieu, D. L'Hôte, and G. Tarjus, Phys. Rev. E **76**, 041510 (2007).
[19] C. Donati, S. C. Glotzer, P. H. Poole, W. Kob, and S. J. Plimpton, Phys. Rev. E **60**, 3107 (1999).
[20] B. Doliwa and A. Heuer, Phys. Rev. E **61**, 6898 (2000).
[21] A. C. Mitus, A. Z. Patashinski, A. Patrykiejew, and S. Sokolowski, Phys. Rev. B **66**, 184202 (2002).
[22] J. C. Crocker and D. G. Grier, Phys. Rev. Lett. **73**, 352 (1994).
[23] K. Kegler, M. Salomo, and F. Kremer, Phys. Rev. Lett. **98**, 058304 (2007).
[24] P. G. Bolhuis, A. A. Louis, J. P. Hansen, and E. J. Meijer, J. Chem. Phys. **114**, 4296 (2001).
[25] A. A. Louis, E. Allahyarov, H. Löwen, and R. Roth, Phys. Rev. E **65**, 061407 (2002).
[26] M. Dijkstra, R. van Roij, and R. Evans, Phys. Rev. E **59**, 5744 (1999).
[27] M. Dijkstra and J. M. Brader, J. Phys.: Condens. Matter **11**, 10079 (1999).
[28] V. Heinonen, A. Mijailovi, C. V. Achim, T. Ala-Nissila, R. E. Rozas, J. Horbach, and H. Löwen, J. Chem. Phys. **138**, 044705 (2013).
[29] G. Yatsenko, E. J. Sambriski, M. A. Nemirovskaya, and M. Guenza, Phys. Rev. Lett. **93**, 257803 (2004).
[30] J. McCarty, I. Y. Lyubimov, and M. G. Guenza, Macromolecules **43**, 3964 (2010).
[31] F. Sagués, J. M. Sancho, and J. García-Ojalvo, Rev. Mod. Phys. **79**, 829 (2007).
[32] M. Majka and P. F. Góra, Acta Phys. Pol. B **43**, 1133 (2012).
[33] M. Majka and P. F. Góra, Phys. Rev. E **86**, 051122 (2012).
[34] M. Majka and P. F. Góra, Acta Phys. Pol. B **44**, 1099 (2013).
[35] M. Chaichian and A. Demichev, *Path Integrals in Physics* (IOP, London, 2001), Vol. I.
[36] J. Dautenhahn and C. K. Hall, Macromolecules **27**, 5399 (1994).
[37] A. A. Louis, P. G. Bolhuis, and J. P. Hansen, Phys. Rev. E **62**, 7961 (2000).

[38] R. Finken, J. P. Hansen, and A. A. Louis, J. Stat. Phys. **110**, 1015 (2003).
[39] R. Kubo, M. Toda, and N. Hashitsume, *Statistical Mechanics I* (Springer, Berlin, 1985).
[40] K. Huang, *Statistical Mechanics* (Wiley, New York, 1987).
[41] C. Hoheisel and R. Zhang, Phys. Rev. A **43**, 5332 (1991).
[42] K. R. Sütterlin, A. Wysocki, A. V. Ivlev, C. Räth, H. M. Thomas, M. Rubin-Zuzic, W. J. Goedheer, V. E. Fortov, A. M. Lipaev, V. I. Molotkov, O. F. Petrov, G. E. Morfill, and H. Löwen, Phys. Rev. Lett. **102**, 085003 (2009).
[43] A. V. Ivlev, S. K. Zhdanov, H. M. Thomas, and G. E. Morfill, Europhys. Lett. **85**, 45001 (2009).